The final publication is available at Springer via http://dx.doi.org/10.1007/s12104-015-9665-4

Chemical Shift Assignments of Calmodulin constructs with EF hand mutations.

Michael Piazza, J. Guy Guillemette and Thorsten Dieckmann [*]

Department of Chemistry, University of Waterloo, Waterloo, Ontario N2L 3G1, Canada

Abstract

Calmodulin (CaM) is a ubiquitous cytosolic Ca^{2+}-binding protein able to bind and regulate hundreds of different proteins. It consists of two globular domains joined by a flexible central linker region. Each one of these domains contains two EF hand pairs capable of binding to Ca^{2+}. Upon Ca^{2+} binding CaM undergoes a conformational change exposing hydrophobic patches that interact with its intracellular target proteins. CaM is able to bind to target proteins in the Ca^{2+}-replete and Ca^{2+}-deplete forms. To study the Ca^{2+}-dependent/independent properties of binding and activation of target proteins by CaM, CaM constructs with Ca^{2+} binding disrupting mutations of Asp to Ala at position 1 of each EF hand have been used. One target protein of CaM is nitric oxide synthase (NOS), which catalyzes the production of nitric oxide (NO). At elevated Ca^{2+} concentrations, CaM binds to neuronal NOS (nNOS) and endothelial NOS (eNOS), making them the Ca^{2+}-dependent NOS enzymes. In contrast, inducible NOS (iNOS) is transcriptionally regulated *in vivo* and binds to CaM at basal levels of Ca^{2+}. Here we report the NMR backbone and sidechain resonance assignments of C-lobe Ca^{2+}-replete and deplete CaM_{12}, N-lobe Ca^{2+}-replete and deplete CaM_{34}, CaM_{1234} in the absence of Ca^{2+} and N-lobe Ca^{2+}-replete CaM_{34} with the iNOS CaM-binding domain peptide.

[*] To whom correspondence should be addressed: Dept. of Chemistry, University of Waterloo, 200 University Ave. W, Waterloo, Ontario N2L 3G1 Canada. Tel. 519-888-4567 ext. 35036; Fax 519-746-0435; E-mail: tdieckma@uwaterloo.ca

Keywords

Calmodulin. Nitric Oxide Synthase. NMR spectroscopy. Resonance assignment.

Biological context

Calmodulin (CaM) is a ubiquitous cytosolic Ca^{2+}-binding protein that is able to bind and regulate hundreds of different proteins (Ikura and Ames 2006). CaM consists of two globular domains joined by a flexible central linker region. Each one of these domains contains two EF hand pairs capable of binding to Ca^{2+}. Each EF hand consists of a helix-loop-helix structural element, with the 12 residues long loop being rich in aspartates and glutamates. Upon Ca^{2+} binding to CaM's EF hands, CaM undergoes a conformational change that exposes hydrophobic patches on each domain thereby allowing CaM to associate with its intracellular target proteins. The central linker's flexibility allows it to adapt its conformation to optimally associate with its intracellular targets (Persechini and Kretsinger 1988). CaM is able to bind to target proteins in the Ca^{2+}-replete and Ca^{2+}-deplete forms.

To study the Ca^{2+}-dependent/independent properties of binding and activation of target proteins by CaM, numerous studies use a series of CaM mutants that involves conversion of Asp to Ala at position 1 of each EF hand (Geiser et al. 1991, Xia et al. 1998, Xiong et al. 2010). Changing the aspartate residue at position 1 of the EF hand loop of CaM inactivates the EF hand toward Ca^{2+} binding. These CaM proteins are defective in Ca^{2+} binding in either the N-terminal lobe EF hands (CaM_{12}; CaM D20A and D56A mutations), the C-terminal lobe EF hands (CaM_{34}; CaM D93A and D129A), or all four of its Ca^{2+}-binding EF hands (CaM_{1234}; mutations at D20A, D56A, D93A and D129A inclusive). A recent study by Xiong et al. (2010) has shown that although conversion of D93 and D129 to Ala effectively inhibits Ca^{2+} binding to EF hands III and IV, the mutations may cause some structural perturbations in the C-domain. This suggests that the Ca^{2+}-deficient CaM mutants may adopt a different structure compared to that of the apo N- and C-domains of CaM.

One of the target proteins bound and regulated by CaM is the nitric oxide synthase (NOS) enzymes. These enzymes catalyze the production of nitric oxide (•NO) that acts as a secondary inter- and intracellular messenger involved in many physiological processes (Alderton et al. 2001). Three NOS isozymes are found in mammals: neuronal NOS (nNOS, NOS I), endothelial NOS (eNOS, NOS III), and inducible (iNOS, NOS II). The NOS enzymes are homodimeric with each monomer containing an

N-terminal oxygenase domain and a *C*-terminal reductase domain, connected by a CaM binding domain (Alderton et al. 2001, Daff 2010). At elevated Ca^{2+} concentrations, CaM binds to and activates the cNOS enzymes, nNOS and eNOS, making them Ca^{2+}-dependent NOS enzymes. In contrast, iNOS is transcriptionally regulated *in vivo* by cytokines and binds to CaM at basal levels of Ca^{2+}. The Ca^{2+}-deficient mutant CaM proteins can be used to allow for a specific structural investigation of Ca^{2+}-dependent/independent activation and binding of CaM to iNOS. Previous to this study the solution structures of apoCaM, holoCaM and holoCaM with the iNOS CaM-binding domain peptide have been determined (Kuboniwa et al. 1995, Piazza et al. 2012).

Here we present the NMR resonance assignments of C-lobe Ca^{2+}-replete and deplete CaM_{12}, N-lobe Ca^{2+}-replete and deplete CaM_{34}, CaM_{1234} in the absence of Ca^{2+} and N-lobe Ca^{2+}-replete CaM_{34} with the iNOS CaM-binding domain peptide. These assignments can be used to solve the solution structures of these Ca^{2+}-deficient CaM mutants and compare them to known structures of apoCaM. Furthermore, these assignments can be used as a foundation for further NMR studies of Ca^{2+}-deficient CaM mutants interacting with various target peptides, such as the NOS peptides.

Methods and experiments

Expression and purification of CaM_{1234}, CaM_{12} and CaM_{34}

Plasmids coding for CaM_{12}, CaM_{34} and CaM_{1234} were subcloned into the kanamycin resistant vector pET9dCaM. The human iNOS (RREIPLKVLVKAVLFACMLMRK, 22 residues corresponding to residues 510-531 from the full length iNOS protein) peptide was synthesized and purchased from Sigma. CaM_{12}, CaM_{34} and CaM_{1234} were expressed in *E. coli* BL21DE3 competent cells and grown in M9 media (11.03 g/L $Na_2HPO_4 \cdot 7H_2O$, 3.0 g/L KH_2PO_4, 0.5 g/L NaCl, 2 mM $MgSO_4$, 0.1 mM $CaCl_2$, 5 mg/mL Thiamine, 100 µg/mL kanamycin) containing 2 g/L ^{13}C-glucose and 1 g/L $^{15}NH_4Cl$ at 37°C. Protein expression was induced at an OD_{600nm} of 0.6 with 500 µM isopropyl-*β*-D-thiogalactopyranoside (IPTG) and harvested after 4 h by centrifugation at 6000 x g at 4°C for 5 minutes. Cells were resuspended in 4 volumes of 50 mM MOPS, 100 mM KCl, 1 mM EDTA, 1 mM DTT, pH 7.5 and lysed by homogenization using an Avestin EmulsiFlex-C5 homogenizer (Ottawa, ON). The lysate was then

clarified by centrifugation at 48,000 x g for 30 minutes at 4°C. To the clarified supernatant, $CaCl_2$ was added to a concentration of 5 mM in order to saturate CaM with Ca^{2+} and induce the exposure of hydrophobic patches in the N- and C-domains of CaM to allow CaM to interact with the resin. This Ca^{2+}-saturated supernatant was then loaded onto 20 mL of phenyl sepharose 6 fast flow highly-substituted resin (GE Healthcare Bio-Sciences, Baie d'Urfe, PQ) in a 1 cm x 30 cm Econo-column (Bio-Rad Laboratories, Mississauga, ON) equilibrated with 50 mM Tris-HCl, 1 mM $CaCl_2$, pH 7.5 @ 4°C. After the Ca^{2+}-saturated solution was loaded; the resin was washed with 100 mL of the above. The resin was subsequently washed with 80 mL of 50 mM Tris-HCl, 500 mM NaCl, 1 mM $CaCl_2$, pH 7.5 @ 4°C to remove any non-specific proteins that were interacting with the resin. The resin was finally washed with 50 mL of 50 mM Tris-HCl, 1 mM $CaCl_2$, pH 7.5 to remove NaCl from the resin. CaM was then eluted from the phenyl sepharose resin with approximately 30 mL of 10 mM Tris-HCl, 10 mM EDTA, pH 7.5 @ 4°C and 2 mL fractions were collected. Fractions were then scanned from 325 to 250 nm on a Varian Cary UV–visible Spectrophotometer (Varian, Mississauga, ON). Fractions displaying the characteristic absorbance peaks of CaM at 277 nm (for tyrosine residues) and 269, 265, 259, and 253 nm (for phenylalanine residues) were pooled and concentrated to 2 mL sample sizes. The samples were then run through a HiLoad 16/600 Superdex 75 column (GE Healthcare Bio-Sciences, Baie d'Urfe, PQ) connected to the Äkta design system (GE Healthcare Bio-Sciences, Baie d'Urfe, PQ) using buffer consisting of 50 mM Tris-HCl, 0.5 mM EDTA, pH 7.5. Fractions eluted at the characteristic time point for proteins of CaM's size were collected. Isolation and purity of the CaM proteins (148 residues) were confirmed by ESI-MS and SDS-PAGE.

NMR spectroscopy

The Ca^{2+} saturated samples were prepared for NMR experiments via a buffer exchange into 100 mM KCl, 10 mM $CaCl_2$, 0.2 mM NaN_3, 90% H_2O/10% ^2H_2O at pH 6.0 using a YM10 centrifugal filter device (Millipore Corp., Billerica, USA). The Ca^{2+} free samples were prepared for NMR experiments via a buffer exchange into 100 mM KCl, 0.5 mM EDTA, 0.2 mM NaN_3, 90% H_2O/10% ^2H_2O at pH 6.0 using a YM10 centrifugal filter device. All NMR samples contained at least 1 mM CaM_{12}, CaM_{34} and

CaM_{1234} in a total volume of 500 µL. The samples were transferred into 5 mm NMR sample tubes and stored at 4°C until required for NMR experiments. NMR experiments on the complexes were conducted on samples titrated with iNOS peptide to saturation in a 1:1 CaM:peptide ratio. Complex formation was monitored after each addition by acquisition of a ^{1}H-^{15}N heteronuclear single-quantum coherence (HSQC) spectrum.

NMR spectra were recorded at 298K on Bruker 600 and 700 MHz DRX spectrometers equipped with XYZ-gradients triple-resonance probes (Bruker, Billerica, MA, USA). Specific NMR resonance assignments were achieved using [^{1}H-^{15}N]-HSQC, HNCA, CBCA(CO)NH, (H)CCH-TOCSY, HC(C)H-TOCSY, ^{13}C-NOESY-HSQC and ^{15}N-NOESY-HSQC experiments, while using the NMR resonance assignments of the wild type CaM as a starting point for the un-mutated lobes of the Ca^{2+}-deficient CaM mutants. Spectra were analyzed using the program CARA (Keller 2005).

Assignments and data deposition

Table 1 shows the list of Ca^{2+}-deficient CaM mutants used in this study, the completeness of their chemical shift assignments and their BMRB accession identification codes. For $apoCaM_{12}$ almost all non-proline backbone resonances were assigned (97.9%) with the exception of A1, D2 and F92. The chemical shift assignment of $apoCaM_{12}$ was deposited in the BMRB database under accession number 26682. $ApoCaM_{34}$ had most non-proline backbone resonances assigned (94.5%) with the exception of residues A1, D2, R90, V91, F92, I100, V136 and E140. The chemical shift assignment of $apoCaM_{34}$ was deposited in the BMRB database under accession number 26683. For the $Ca^{2+}CaM_{12}$ construct 97.9% of non-proline backbone resonances were assigned excluding A1, D2 and A57. The chemical shift assignment of $Ca^{2+}CaM_{12}$ was deposited in the BMRB database under accession number 26685. For $Ca^{2+}CaM_{34}$ all non-proline backbone resonances were assigned (91.8%) with the exception of A1, D2, E67, M72, R86, R90, V91, F92, A93, I100, V136 and E140. The chemical shift assignment of $Ca^{2+}CaM_{34}$ was deposited in the BMRB database under accession number 26686.

Figure 1A shows the [^{1}H,^{15}N]- HSQC spectrum of the CaM_{1234}. Almost complete amide resonance assignment for $apoCaM_{1234}$ was achieved. Overall 97.2% of all $^{1}H^{N}$, ^{15}N resonances were assigned with

the exception of the first residue A1, and D2, R90, I100 and the two Proline residues. Among the backbone resonances, 96.6% of Cα, 90.5% of Cβ, and 96.6% of Hα were assigned. In total, 84.0% of sidechain ^{1}H resonances, with 91.9% of Hβ resonances were assigned. Overall, the [^{1}H, ^{15}N] HSQC spectrum exhibits good resolution and well dispersed signals, indicating a uniform and folded protein structure. Chemical shift changes induced by the 4 EF hand mutations appear for the amides throughout all 4 of the Ca^{2+}-binding EF hands, with the greatest differences occurring for the amides in the center of the Ca^{2+}-binding loop (Fig. 2A). The amide resonances of the loop region between EF hands I and II and the linker region between EF hands II and III show little chemical shift differences with each other suggesting a similar structure for both proteins. The chemical shift assignment of apoCaM_{1234} was deposited in the BMRB database under accession number 26681.

Figure 1B shows the [^{1}H,^{15}N]- HSQC spectrum of $Ca^{2+}CaM_{34}$ bound to the iNOS CaM binding domain peptide. Almost complete amide resonance assignment was achieved. Overall 98.6% of all $^{1}H^{N}$, ^{15}N resonances were assigned with the exception of the first A1 residue, I100 and the two Proline residues. Among the backbone resonances, 97.3% of Cα, 96.4% of Cβ, and 97.3% of Hα were assigned. In total 89.4% of sidechain ^{1}H resonances, with 96.4% of Hβ of resonances were assigned. Overall, the [^{1}H, ^{15}N] HSQC spectrum exhibits good resolution and well dispersed signals, indicating a uniform and folded protein structure. Chemical shift changes induced by the C-lobe EF hand mutations appear for the amides in the C-domain, specifically the amides of residues that participate in coordinating the Ca^{2+} ion in EF hands III and IV, with the greatest differences occurring for the amides in the center of the Ca^{2+}-binding loop (Fig. 2D). The amide resonances of the N-lobe show little chemical shift differences suggesting a similar structure of the N-lobe bound to iNOS for both complexes. The chemical shift assignment of CaM_{34} with iNOS was deposited in the BMRB database under accession number 26687.

The chemical shift changes induced by Ca^{2+} binding to apoCaM_{12} occur for residues only in the C-lobe. This lobe contains the EF hands not affected by mutation and thus still able to undergo the conformational change associated with binding Ca^{2+}. The N-lobe residues show little chemical shift differences indicating a similar structure for the N-lobe in both proteins (Fig. 2B). A similar result is

found with Ca^{2+} binding to apoCaM_{34}, however, in the opposite lobes (Fig. 2C). Tiny chemical shift differences are seen for the C-lobe and large chemical shift differences are seen for the N-lobe.

References

Alderton, W., Cooper, C., Knowles, R. (2001) Nitric oxide synthases: Structure, function and inhibition. Biochem. J. 357: 593− 615.

Daff, S. (2010) NO synthase: Structures and mechanisms. Nitric Oxide 23: 1−11.

Geiser, J., van Tuinen, D., Brockerhoff, S., Neff, M.M., Davis, T.N. (1991) Can calmodulin function without binding calcium? Cell 1991 65: 949-959.

Ikura, M., and Ames, J. (2006) Genetic polymorphism and protein conformational plasticity in the calmodulin superfamily: Two ways to promote multifunctionality. Proc. Natl. Acad. Sci. U.S.A. 103: 1159−1164.

Keller, R. (2005) Optimizing the Process of Nuclear Magnetic Resonance Spectrum Analysis and Computer Aided Resonance Assignment. Dissertation, Swiss Federal Institute of Technology, Zurich.

Kuboniwa, H., Tjandra, N., Grzesiek, S., Ren, H., Klee, C., Bax, A. (1995) Solution structure of calcium-free calmodulin. Nat. Struc. Biol. 2: 768-776.

Persechini, A., and Kretsinger, R. (1988) The central helix of calmodulin functions as a flexible tether. J. Biol. Chem. 263: 12175− 12178.

Piazza, M., Futrega, K., Spratt, D., Dieckmann, T., Guillemette, G. (2012) Structure and Dynamics of Calmodulin (CaM) Bound to Nitric Oxide Synthase Peptides: Effects of a Phosphomimetic CaM Mutation. Biochem. 51: 3651-3661.

Xia, X. Fakler, B., Rivard, A., Wayman, G., Johnson-Pais, T., Keen, J., Ishii, T., Hirshberg, B., Bond, C., Lutsenko, S., Maylie, J., Adelman, J. (1998) Mechanism of calcium gating in small-conductance calcium-activated potassium channels. Nature 395: 503-507.

Xiong, L., Kleerekoper, Q., Wang, X., Putkey, A. (2010) Intra- and interdomain effects due to mutation of calcium-binding sites in calmodulin. J. Biol. Chem. 285: 8094-8103.

Table 1. Ca^{2+}-deficient CaM mutants used in this study and completion of chemical shift assignments.

CaM mutant	Nuclei assigned	% Backbone assigned	% Sidechain assigned	Residues missing[a]	BMRB #
$ApoCaM_{12}$	H, NH	97.9	N/A[b]	A1, D2, F92	26682
$ApoCaM_{34}$	H, NH	94.5	N/A[b]	A1, D2, R90, V91, F92, I100, V136, E140	26683
$Ca^{2+}CaM_{12}$	H, NH	97.9	N/A[b]	A1, D2, A57	26685
$Ca^{2+}CaM_{34}$	H, NH	91.8	N/A[b]	A1, D2, E67, M72, R86, R90, V91, F92, A93, I100, V136, E140	26686
$ApoCaM_{1234}$	H, NH, Cα, Cβ, Hα, Hβ, Hγ, Hδ	97.2	96.6 Cα, 90.5 Cβ, 84.0 sidechain H, 96.6 Hα, 91.9 Hβ	A1, D2, R90, I100	26681
$Ca^{2+}CaM_{34}$-iNOS	H, NH, Cα, Cβ, Cγ ,Cδ , Hα, Hβ, Hγ, Hδ	98.6	97.3 Cα, 96.4 Cβ, 89.4 sidechain H, 97.3 Hα, 96.4 Hβ	A1, I100	26687

[a]Chemical shifts were not assigned for P43 or P66.

[b]Experiments to assign sidechain nuclei were not acquired.

.

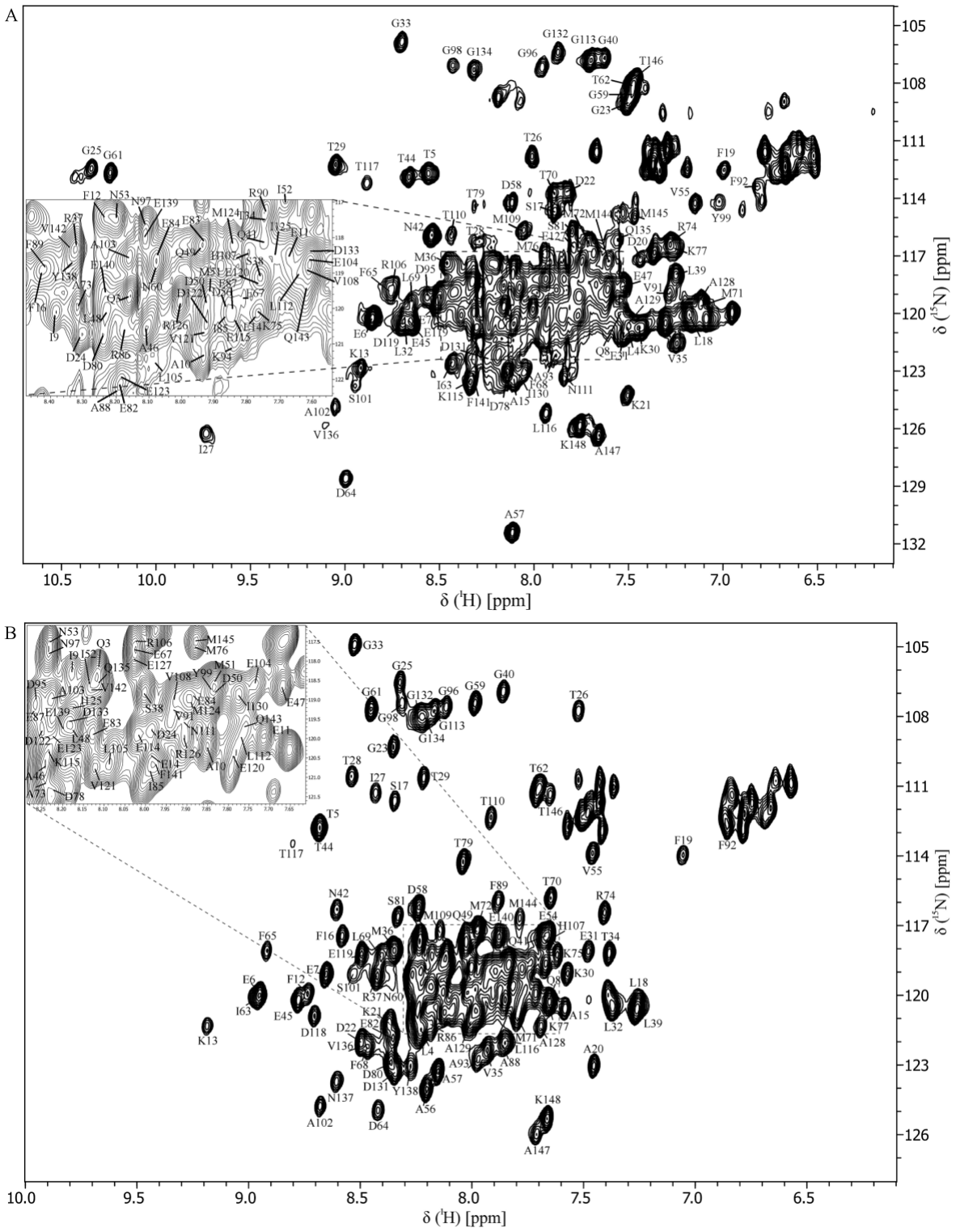

Fig. 1

(A) [^{1}H,^{15}N]-HSQC spectrum of CaM_{1234}. (B) [^{1}H,^{15}N]-HSQC spectrum of CaM_{34} bound to the iNOS CaM binding domain peptide. Each backbone amide resonance is labeled with the amino acid type and position in the sequence.

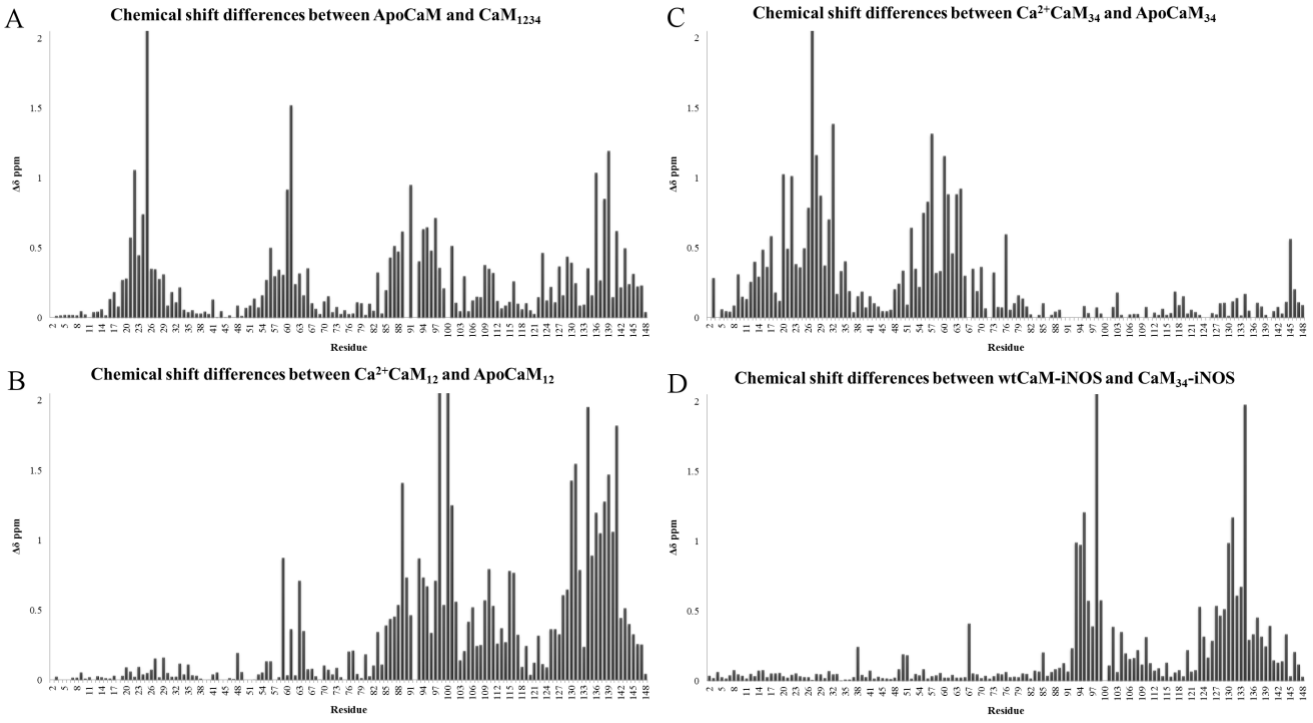

Fig. 2

Chemical shift differences between: (A) ApoCaM and CaM_{1234}; (B) Apo and $Ca^{2+}CaM_{12}$; (C) Apo and $Ca^{2+}CaM_{34}$; and (D) wt CaM−iNOS complex and CaM_{34}−iNOS complex. The contribution of ^{1}HN and ^{15}N chemical shift changes for each residue was calculated as $\Delta\delta = \sqrt{[(\Delta\delta^{1}HN)^2 + (\Delta\delta^{15}N/5)^2]}$, where $\Delta\delta^{1}HN$ and $\Delta\delta^{15}N$ are the differences in ^{1}HN and ^{15}N chemical shifts between the indicated protein. The greatest differences are localized to Ca^{2+} binding loops where each mutation is present.